SODIUM INACTIVATION

EXPERIMENTAL TEST OF TWO MODELS

ROSALIE C. HOYT *and* WILLIAM J. ADELMAN, JR.

From the Department of Physics, Bryn Mawr College, Bryn Mawr, Pennsylvania 19010, the Department of Physiology, The University of Maryland School of Medicine, Baltimore, Maryland 21201, and the Marine Biological Laboratory, Woods Hole, Massachusetts 02543

ABSTRACT Analyses of inactivation experiments performed on unperfused axons of the squid have been compared with the predictions of the Hodgkin-Huxley and the Hoyt mathematical models for the early (sodium) conductance. The results are in good agreement with the latter and in disagreement with the former.

INTRODUCTION

The time and voltage dependence of the early (sodium) conductance of the giant axon of the squid have been quantitatively fitted, for normal environmental conditions, to two different mathematical descriptions or models. In the model developed by Hodgkin and Huxley (1952), the conductance is dependent on the product of two independent variables, m^3 and h, while in the model developed by Hoyt (1963) the conductance depends on only one variable, v, but v is determined by two coupled processes. While these two models give indistinguishable predictions for most experimental phenomena, it was shown in an earlier publication, Hoyt (1968), that the coupled model predicts a dependence of inactivation curves on the test potential while the Hodgkin and Huxley (HH) independent variable model predicts that inactivation curves should be essentially invariant with respect to the test potential. A search of the literature revealed at that time few published experiments that could be used to put the two models to a comparative test. Additional experiments were therefore performed at Woods Hole during the summer of 1967. The results of these experiments and their analyses are presented below.

METHODS

Experimental

Experiments were performed upon single giant axons of *Loligo pealei* during the summer of 1967 at the Marine Biological Laboratory, Woods Hole, Mass. The methods of preparation and the voltage clamp system have been previously described (Adelman and Senft, 1968; Adelman and Palti, 1969). All experiments were carried out at a temperature of 3 ± 2°C. The artificial sea water consisted of the following: 430 mM NaCl, 10 mM KCl, 10 mM $CaCl_2$, 50 mM $MgCl_2$, 0.5 mM Tris buffer.

Analytical

It is well known that the peak early currents, I_p, are dependent on both the test potential, E_t, and the conditioning potential, E_c, i.e.,

$$I_p = f(E_t, E_c).$$

Two methods can, therefore, be used to present these dependencies: a set of $I_p(E_t)$ curves at different fixed E_c values (Fig. 1 *a*), and a set of $I_p(E_c)$ curves at different fixed E_t values (Fig. 1 *b*). These two sets of curves are interrelated; either one may be derived from the other. For example, if a vertical line is passed through the curves on the left, at fixed E_t, and the points read off, one of the curves on the right is obtained (1, 2, 3, 4, 5). Similarly, if a vertical line is passed through the curves on the right, at fixed E_c, one of the curves on the left is obtained (a, b, c, d, e). The conditioning curves of Fig. 1 *b* were of particular interest in this study, yet the data were often more conveniently taken in the primary form of Fig. 1 *a*. By passing smooth curves through the experimental points, a number of conditioning curves could be constructed by reading off at different vertical, E_t = constant, lines. The curves of Fig. 1 are schematic only and no particular significance should be given to their particular shape.

Although the primary data obtained were peak early *currents* (corrected for leakage), it is more convenient to consider peak sodium *conductances* by making the ohmic assumption of Hodgkin and Huxley,

$$I_p = (E_t - E_{Na})g_p,$$

where E_{Na} is the sodium reversal potential and g_p is the peak sodium conductance. While direct calculation of $g_p = I_p/(E_t - E_{Na})$ is possible, it requires an experimental determination of E_{Na}, i.e., that value of E_t that gives $I_p = 0$. An analytic method that does not require knowledge of the sodium reversal potential but also is based on the ohmic assumption, con-

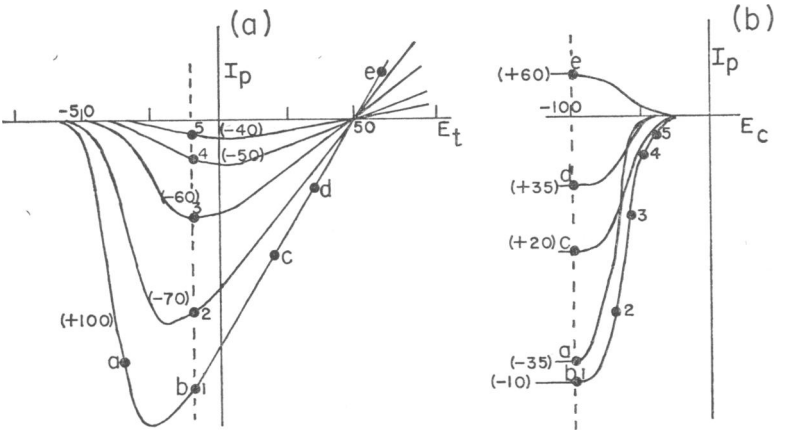

FIGURE 1 Two ways of presenting the $I_p(E_t, E_c)$ functional relationships. (*a*) Constant E_c curves; the numbers in parenthesis give the E_c values. (*b*) Constant E_t curves; the numbers in parenthesis give the E_t values. The numbered and lettered points indicate the interrelationship between the two sets of curves (see text).

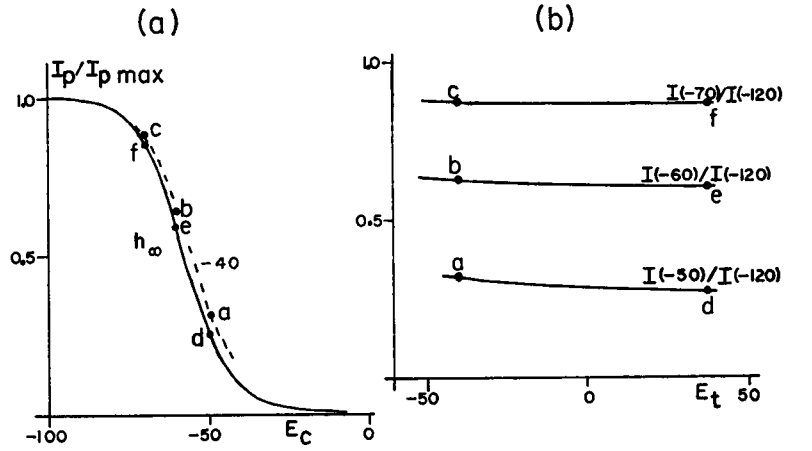

FIGURE 2 Predictions of the HH (1952) model. The absolute voltage scales, expressed in millivolts, were obtained by assuming arbitrarily a resting potential of −60 mv. (*a*) Normalized inactivation curves. Solid curve: the h_∞ parameter; this curve is also valid for test potentials more positive than −20 mv. Dashed curve: inactivation curve for E_t = −40 mv. (*b*) Dependence on test potential of normalized peak current ratios for E_c values of −70 mv, −60 mv, and −50 mv. The lettered points indicate the interrelationship between the two sets of curves.

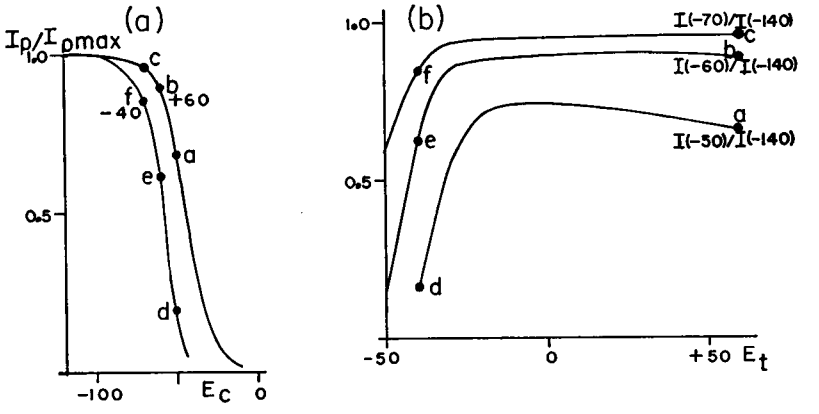

FIGURE 3 Predictions of the Hoyt (1963) model. The absolute voltage scales, expressed in millivolts, were obtained by assuming arbitrarily a resting potential of −60 mv. (*a*) Normalized inactivation curves for E_t = −40 mv and +60 mv. (*b*) Dependence on test potential of normalized peak current ratios for E_c values of −70 mv, −60 mv, and −50 mv. The "sharpened," w_∞', curve of Fig. 6 *c* of Hoyt (1968) was used for these calculations. The lettered points indicate the interrelationship between the two sets of curves.

sists of computing peak current *ratios* (corrected for leakage) at fixed E_t, since these should give the corresponding peak conductance *ratios*. Such ratios are most conveniently normalized by dividing the I_p value at any E_c by the maximum I_p obtained at a large hyperpolarizing E_c value, both, of course, taken at the same E_t value. Two methods of presenting these ratios

will be used here. The first is the conventional one of plotting the normalized ratios against E_c, with fixed E_t, the so-called "inactivation curves" (Figs. 2 *a* and 3 *a*). In the second method these ratios (at same E_t) are plotted against E_t, using fixed E_c values (Figs. 2 *b* and 3 *b*).

Before presenting the experimental curves we shall indicate, for both methods of presentation, the predictions of the two models under consideration. The predictions of the HH (1952) mathematical model are shown in Fig. 2, those of the Hoyt model (1963 and 1968) are shown in Fig. 3. As shown in Fig. 2 *a*, the HH model predicts, for all test potentials greater than −20 mv, that the inactivation curves should follow very closely the h_∞ curve, and thus be essentially independent of the test potential used. At very small test voltages ($E_T < -30$ mv), the HH equations predict a slight broadening of the curve (dashed curve of Fig. 2 *a*). As discussed and analyzed in an earlier paper (Hoyt, 1968), this broadening results from a breakdown of two approximations that are normally made: (*a*) that the equilibrium value of h at the test potential is negligibly small, and (*b*) that the equilibrium value of m at the conditioning potential is negligibly small. For test potentials only slightly depolarizing ($E_T < -30$ mv), the first approximation breaks down, and for conditioning potentials only slightly hyperpolarizing ($E_c > -60$ mv), the second approximation breaks down. It is the breakdown of these two approximations that leads, according to the HH equations, to the prediction of a slight broadening (or a shift to the right) as the test potential is made less depolarizing.

An alternative method of presenting these same predictions is shown in Fig. 2 *b*. Peak current ratios are here displayed as functions of the test potential at constant conditioning potential, rather than as functions of the conditioning potential at constant test potential. The interrelationship of Figs. 2 *a* and 2 *b* is perhaps made clearer by inspection of the six labeled data points (a, b, c, d, e, f) as they are plotted in the two different ways.

The predicted invariance of the inactivation curve at large test potentials in Fig. 2 *a* shows up in the horizontal flatness of the curves of Fig. 2 *b* at large test potentials, while the slight broadening at small test potentials in Fig. 2 *a* (dashed curve) shows up as slightly increasing values as one moves to the left in Fig. 2 *b*.

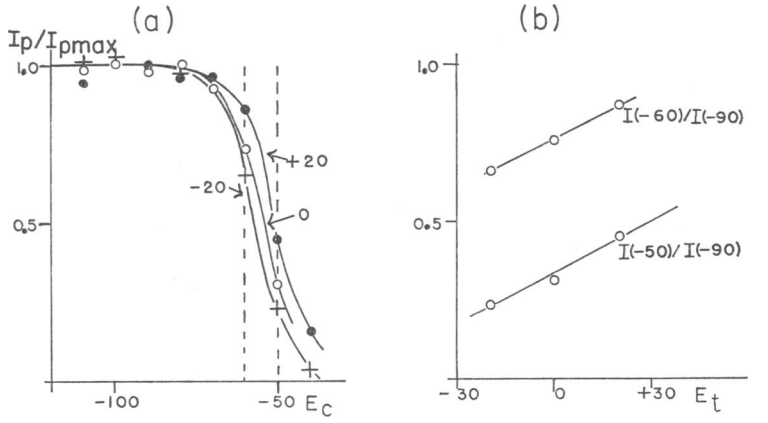

FIGURE 4 Experimental peak current ratios for axon No. 67–5. All voltage scales are in millivolts. (*a*) Inactivation curves. Crosses: $E_t = -20$ mv; open circles: $E_t = 0$ mv; filled circles: $E_t = +20$. The conditioning potentials were about 2 sec in duration. (*b*) Peak current ratios read off the two dashed vertical lines in Fig. 4 *a* at $E_c = -60$ mv and −50 mv.

A distinctly different behavior is predicted by the Hoyt model, as shown in Fig. 3. With decreasing test potentials the inactivation curves (Fig. 3 *a*) are shifted to the left rather than to the right as in the HH model, and the shifts are quite appreciable in magnitude. (Note the difference in voltage scales of Figs. 2 *a* and 3 *a*.) These large shifts show up in Fig. 3 *b* as rapid decreases in the ratio values as the test potential is reduced below −20 mv, rather than the very small increases predicted by the HH model.

Since the predictions of Figs. 2 and 3 are both qualitatively and quantitatively different, experimental tests should be feasible. The results of such experimental tests are given in the next section.

RESULTS

The set of experimental inactivation curves shown in Fig. 4 *a* is typical of those obtained with several axons. It is obvious that these curves are shifted to the left

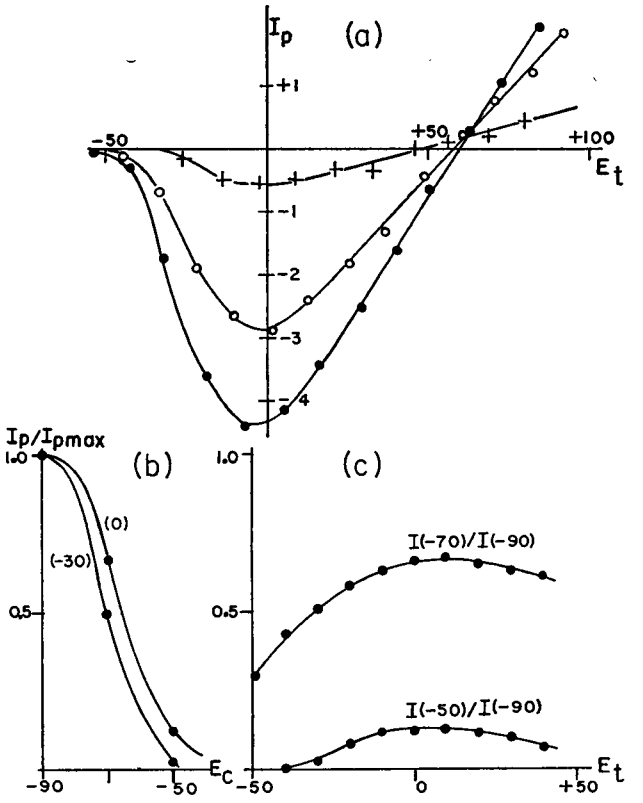

FIGURE 5 Peak currents and peak current ratios for axon No. 67-26. All voltage scales are in millivolts. (*a*) Peak current curves. Crosses: $E_c = -50$ mv; open circles: $E_c = -70$ mv; filled circles: $E_c = -90$ mv. The conditioning potential was the holding potential in each case. The current scale is in ma/cm². (*b*) Conditioning curves at $E_t = -30$ mv and 0 mv obtained from curves in Fig. 5 *a*. (*c*) Dependence on test potential of peak current ratios obtained from curves in Fig. 5 *a*.

as the test potential is made less depolarizing, a behavior similar to that of Fig. 3 *a*, not to that of Fig. 2 *a*. Points read off these curves along the two dashed vertical lines are plotted against the corresponding E_t value in Fig. 4 *b*. Again, the fall with decreasing E_t is similar to the behavior of Fig. 3 *b*, not to that of Fig. 2 *b*.

Typical curves of the peak current vs. test potential curves obtained with a number of axons are those shown in Fig. 5 *a*. Using the smooth curves fitted to the experimental points, the ratios $(I_p)_{-70}/(I_p)_{-90}$ and $(I_p)_{-50}/(I_p)_{-90}$ were calculated at a number of E_t values. These ratios are plotted, where the subscripts refer to the (E_c values, both as functions of E_c at fixed E_t, and as functions of E_t at fixed E_c in Figs. 5 *b* and *c*, respectively. Again the behavior is seen to be quite similar to that shown in Fig. 3 and to be distinctly different from that shown in Fig. 2.

Finally, in Fig. 6 ratios are plotted against E_t for a number of other axons, all in agreement with the predictions of Fig. 3 *b*. All of the plots in Fig. 6 were derived

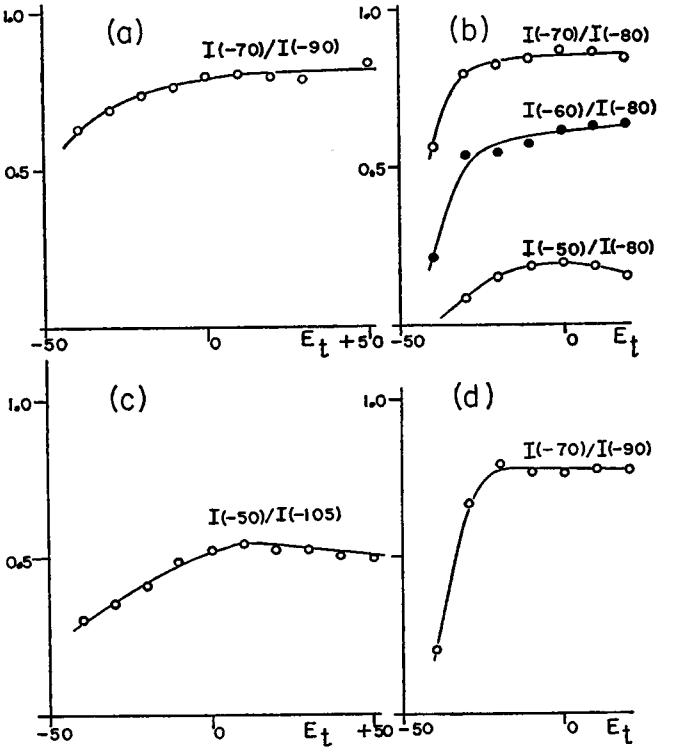

FIGURE 6 Dependence on test potential of the peak current ratios at two different conditioning potentials. All voltage scales are in millivolts. For the curves in Figs. 6 *a*, *b*, and *d*, the conditioning potential was the holding potential. For the curve in Fig 6 *c* the axon was held at $E_H = -70$ and prepulsed for 25 msec to the conditioning potential. Curves in Figs. 6 *a* and *c*: axon No. 67-22. Curve in Fig. 6 *b*: axon No. 67-33. Curve in Fig. 6 *d*: axon No. 67-24.

from peak current vs. test potential curves at two or more different conditioning potentials, curves similar to those of Fig. 5 *a*. For all except the curve of Fig. 6 *c*, the conditioning potential was the holding potential. Since data obtained in this way require that the holding potential be maintained for considerable times, up to several minutes, long term effects dependent on the holding potential might distort the results. This was one of the unanswered questions raised earlier in the analysis of the Adelman and Fok (1964) axon No. 63–76 (Hoyt, 1968). That no such long term effects due to the holding potential are affecting the curves presented here is shown by the behavior of the curve of Fig. 6 *c* in which 25-msec conditioning prepulses from a fixed holding potential of −70 mv were used. The curve of Fig. 6 *c* is seen to be similar in behavior to all the other presented here, indicating that holding for several minutes and prepulsing for 25 msec yield similar results.

DISCUSSION

The results presented above give a clear indication that the coupled equations kinetics of the Hoyt model are better able to describe inactivation phenomena in the unperfused axon, when ASW is used as the external solution, than those of the independent n and h variables of the HH model. No study of the perfused fiber was made here. However, behavior similar to that illustrated in Fig. 4 *a* was found in the earlier study (Hoyt, 1968), of the Adelman and Fok (1964) perfused axon No. 63–76 in which a perfusion fluid of 33 mM K + sucrose, and external ASW, were used, allowing the above conclusion to be generalized to perfused fibers as well, even those with somewhat low internal ionic strength. It was also shown in the earlier study that a similar conclusion can probably be drawn for *Xenopus* nodes. Finally, confirmation is now given to the tentative conclusion drawn earlier (Hoyt, 1968), with regard to the results published by Chandler and Meves (1965) in which two inactivation curves at test potentials of −11 and +97 mv were shown to be identical. This merely requires that the ratio curves be flat for test potentials greater than −11 mv (Fig. 3 *b*).

The flatness referred to above was often (Fig. 6 *d*), but not always, observed in the present study. A droop was sometimes observed at large test potentials, especially at the more depolarizing conditioning potentials. This effect can be predicted by the Hoyt model (Fig. 3 *b*) and results from an increase in the rate constant ratio, k_3/k_1, with increasing test potential. An experimental example is shown in Fig. 5 *c*, although part of this droop probably results from the shift of E_{Na} that often is observed at the more depolarizing conditioning potentials.

Although predictions of only the Hoyt model were shown in Fig. 3, it was noted earlier (Hoyt, 1968), that qualitatively similar results are to be expected from other coupled equation models such as those of Goldman (1964) and Mullins (1960). We thus conclude in general that coupled equation models for the early conductance fit the experimental inactivation behavior of axons better than do independent variable models such as that of Hodgkin and Huxley. In particular, the Hoyt model

is found to give a very close fit to the axon data, while that of Hodgkin and Huxley departs considerably from the observed inactivation behavior. These conclusions imply that the mechanism responsible for the increase in sodium conductance is more likely to be dependent on the production of an intermediate state than on the competition of two antagonistic but independent processes such as the movements of the HH activating and inactivating particles. If the idea of an intermediate active state (coupled to two or more other inactive states) is indeed correct, as our analyses suggest, no choice can be made at this time between the many possible mechanisms of this type (rotation of dipole groups; binding and disassociation of two or more ionic species; a combination of dipole rotation and ionic binding and disassociation; etc.).

Although the HH and Hoyt mathematical models for the early conductance changes are qualitatively quite different, their predictions for most phenomena have been strikingly similar. Only in the dependence of inactivation effects on test potential, analyzed here, has a method been found to distinguish between their predictions. Recently Adelman and Palti (1969) have found that both the shape of the inactivation curves and the inactivation time constant are affected by changes in the potassium content of the external solution, $[K_o]$. While effects such as these cannot be used to distinguish between the two models, it is of interest to compare the nature of the modifications required of each model. These modifications have been analyzed for the HH model by Adelman and Palti, and consist primarily of an increase of τ_h and a decrease of h_∞ values with increasing $[K_o]$. For the Hoyt (1963, 1968) model analogous modifications are required, namely a decrease in relative u_∞ (or w_∞) values and a decrease of the rate constant k_3 (or an increase in the time constant $1/k_3$) with increasing $[K_o]$. An accompanying reduction of relative v_∞ values may also be required. The discussion of Adelman and Palti as to the physical mechanism that might be responsible for the changes applies equally well to the Hoyt model.

This work was done with the technical assistance of Richard Marsh and Susan Cree Powers.

This work was supported by United States Public Health Service, National Institutes of Health Grants Nos. NB-04601 and NB-7285.

Received for publication 23 January 1970.

REFERENCES

ADELMAN, W. J., JR., and Y. B. FOK. 1964. *J. Cell. Comp. Physiol.* **64**:429.
ADELMAN, W. J., JR., and Y. PALTI. 1969. *J. Gen. Physiol.* **53**:685.
ADELMAN, W. J., JR., and J. P. SENFT. 1968. *J. Gen. Physiol.* **51** (5, Pt. 2):102s.
CHANDLER, W. K., and H. MEVES. 1965. *J. Physiol. (London).* **180**:788.
GOLDMAN, D. E. 1964. *Biophys. J.* **4**:167.
HODGKIN, A. L., and A. F. HUXLEY. 1952. *J. Physiol. (London).* **117**:500.
HOYT, R. C. 1963. *Biophys. J.* **3**:399.
HOYT, R. C. 1968. *Biophys. J.* **8**:1074.
MULLINS, L. J. 1960. *J. Gen. Physiol.* **43**: (5, Pt. 2):105.